Image blurring of the test section boundary in a laser specklegram technique measuring temperature gradients of the compressible medium

K. D. Kihm
Department of Mechanical Engineering, Texas A&M University, College Station, Texas 77843-3123.
Received 4 February 1992.
0003-6935/92/285907-04$05.00/0.

Image blurring of the solid boundary of a test section has been investigated for a specklegram technique that nonintrus*iuely measures temperature gradients in transparent media.*

A laser specklegram or speckle photography technique enables the direct nonintrusive measurement of temperature gradients for optically thin media with nonuniform refractive-index fields.[1] Optical speckles have resulted from the enhancement or cancellation of collimated light rays scattered through ground glass, and these speckles will be dislocated when a nonuniform temperature or density field is placed in the field of view. The amount of this dislocation is then correlated with the index of refraction variations in the test field.[2] Recent applications[3,4], have shown that the specklegram technique can be a much more accurate and convenient measurement technique for convective heat transfer problems than more classical techniques such as thermocouple probes or mass transfer analogies. One of the most distinctive advantages of the specklegram technique is the capability of the nonintrusive measurement of wall temperature gradients to provide direct information on heat transfer correlation coefficients.

Figure 1 presents an optical arrangement of a specklegram system that has been used for natural convection heat transfer problems by the author.[3,4] A 35-mW He-Ne laser beam was expanded to 125 mm in diameter on the first parabolic mirror, collimated to form a cylindrical probe beam passing the test section, and then focused onto the granular surface of the ground glass that was used to generate optical speckles. The specklegram is obtained by photographically superimposing the speckle images with and then without the test field so that the speckles formed with and without refractions can be recorded. Several variations of specklegram configurations may be available by altering the arrangement of the primary optical elements.s Figures 2 and 3 present schematic ray diagrams for two representative configurations depending on whether the ground glass plate is placed after or before the test section, respectively. The image boundary of a test section on the specklegram may be blurred especially when the ground glass is placed after the test section. This defocused image results in the uncertainties for the solid wall locations and may also bias the wall-temperature-gradient measurements. The image blurring of the solid boundary has been characterized for the two representative speckle gram configurations presented in Figs. 2 and 3. Another factor, such as the thickness of a glass window, has also been inspected.

For both configurations presented in Figs. 2 and 3 the index-of-refraction gradient can be correlated' with other optical parameters as

$$\frac{\partial n}{\partial y} = \frac{\Delta}{c}\frac{n_x}{L}\frac{m}{m'}, \tag{1}$$

where n and n_x denote the index of refraction inside and outside the thermal boundary layer, respectively, y is the coordinate perpendicular to both the solid boundary and the optical axis, Δ represents the amount of the speckle dislocation on the specklegram, c is the defocusing distance measured from the ground glass, L is the overall length of the test section measured in parallel to the beam passage, and m and m' represent the magnification of the (second parabolic) schlieren mirror and the camera, respectively. Substituting the Gladstone-Dale relationship $n = K \times \rho + 1$, where ρ is the gas density in kg/m^3 and K is the Gladstone-Dale constant (for air at a temperature of 288 K, $K = 0.2257 \times 10^{-3}$ m^3/kg for X = 632.8 nm of a He-Ne laser sources), into Eq. (1) provides an expression correlating the temperature gradient to the speckle dislocation:

$$\frac{\partial T}{\partial y} = -\frac{\Delta}{c}\frac{n_x}{L}\frac{m}{m'}\frac{RT^2}{Kp} \tag{2}$$

where an ideal gas medium is assumed, R is a gas constant, and p and T refer to the local pressure and temperature of the medium, respectively. The last fractional expression on the right-hand side of Eq. (2) can be approximated as a constant when the temperature range is moderate.[7]

For the case of a ground glass placed after the test section (Fig. 2) the speckle dislocation is expressed as

$$\Delta = (m'/m) \times c \times \alpha, \tag{3}$$

where α is the refraction angle of light rays in the test field. Optical alignment of the system is necessary to ensure that the test section image is focused properly onto the ground glass. The camera focusing plane for the specklegram recording, however, must be slightly away from the ground glass plane, since the speckle dislocations are not detectable on the ground glass. This defocusing may result in spatial uncertainties of the solid boundary of the test object and could also bias the wall-temperature-gradient data. The amount of the defocusing therefore must be minimized to obtain a wall temperature gradient that is within acceptable accuracy intervals. At the same time the minimization of the defocusing is limited, since if the defocusing distance is too small the speckle dislocation [Eq. (3)] becomes less distinguishable, and the signal-to-noise ratio of the data will be too low.

The amount of the image blur on the specklegram is expressed as ε x h, and the image blur ratio a can be derived from considering the geometry and the Gaussian lens

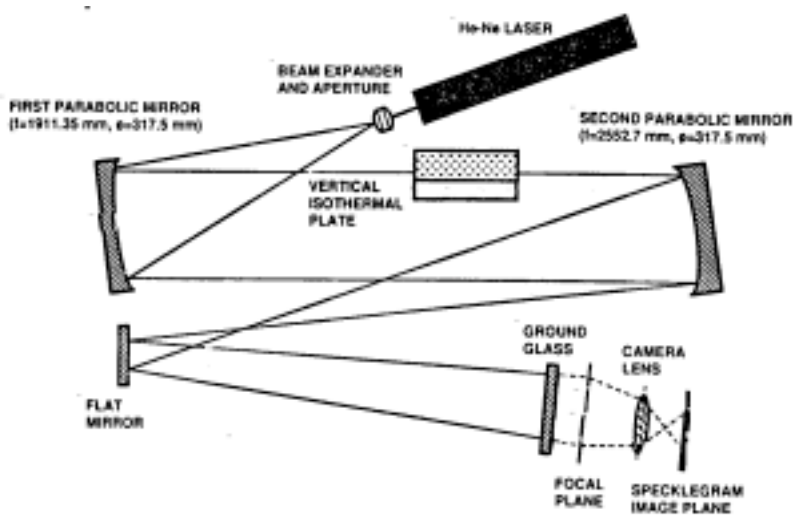

Fig.1 Schematic illustration of the specklegram system.

formula:

$$\varepsilon = \varepsilon_1 + \varepsilon_2 = c\left(\frac{1}{a} + \frac{1}{b}\right)m' \quad , \tag{4}$$

where subscripts 1 and 2 represent the primary and secondary image blur, as indicated in Fig. 2. The secondary blur will be less distinctive since it is somehow mixed with the depth-of-field uncertainty, and the primary blur is expected to make a dominant contribution to the overall image uncertainties. In principle the image can be free from blur when h is equal to zero or for very small objects placed on the optical axis. The image blur, however, will not be completely avoidable for most practical cases of object sizes comparable with the schlieren mirror dimension.

To minimize the image blur the measurement section must be placed near the optical axis to the extent possible. The increasing object distance a reduces the primary blur ratio but enhances the secondary blur because of the decrease in *b* to satisfy the relationship 1 */a + 1 /b = 1 / f* for a given *f* and vice versa for the case of increasing the image distance *b*. Both the primary and secondary blur ratios decrease with the increasing focal length of the schlieren head. The oversized mirrors with long focal lengths are recommended for use for the schlieren head mirror. When the primary blur is minimized by maximizing *a* the magnification of the schlieren head m *(= b/a)* reaches a minimum for a given *f* and c, and the speckle dislocation expressed in Eq. (3) is maximized. Therefore, as long as the secondary blur does not significantly influence the data biasing, the maximization of a contributes to reducing the image blur as well as to enhancing the speckle dislocations or the signalto-noise ratio.

The relative measurement position to the total length of the test section E must be small to minimize a line-of-sight bias occurring from a multiple refraction of rays, especially for the case of a steep temperature gradient. Values of ξ

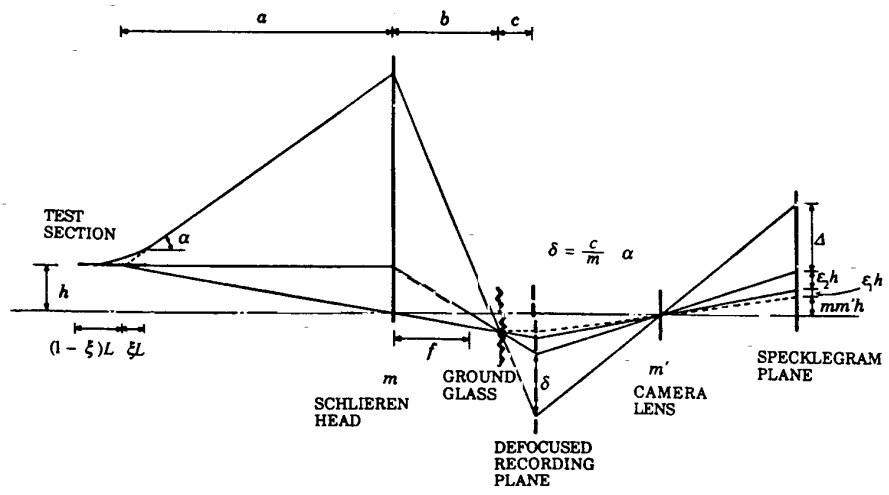

Fig. 2. Schematic configuration of a specklegram system with a ground glass placed after a test section.

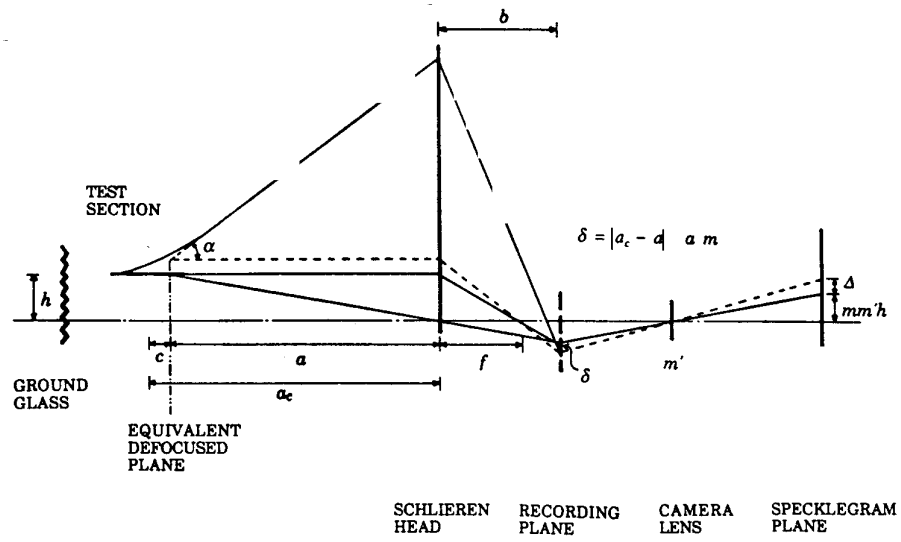

Fig. 3. Schematic configuration of a specklegram system with a ground glass placed before a test section.

ranging from 0.1 to 0.4 are recommended from previous applications of the technique.3.[3,4] If ξ is smaller than 0.1, the edge effect may bias the data.

For the increasing camera magnification m', the signal-to-noise ratio will be enhanced with increasing speckle dislocations on the specklegram, but the image blur ratio will also be increased. An ideal magnification in practice is determined usually by a trial-and-error procedure incorporating other technical aspects such as the film speed (photochemical grain sizes), the exposure time, the laser source power output, and the camera lens aperture.

A sample calculation has been made for the image blur for the specklegram configuration employed in the previous work,[4] and the total image blur ratio a given by Eq. (4) is evaluated to be 7.86 x 10^{-3} (a = 570 cm, b = 460 cm, c = 2.5 cm, f = 255 cm, m = 0.8, and m' = 0.8 in Fig. 2) with the primary blur ratio ε_1 = 3.51 x 10^{-3} and the secondary blur ratio ε_2 = 4.35 x 10^{-3}. For a test object extending 50 mm in length from the optical axis, for example, the total image blur in the worst situation can be up to 0.4 mm on the specklegram and up to 0.62 mm in the physical scale. Other aspects such as optical as well as photographic imperfections may increase the overall blur ratio.

When the ground glass is placed ahead of the test section (Fig. 3), optical speckles are formed before the test section. The refraction angle a is usually very small (of the order of 10^{-5} rad), and the speckle dislocations can be obtained from the following geometry:

$$\Delta = m \times m' \times c \times \alpha, \tag{5}$$

where the equivalent defocusing length c is given as the length between the center of the test section and the actual object distance of the schlieren head $|a_c - a|$. The main distinction in the configuration in Fig. 3 is that the speckles are formed and dislocated inside the test section and the dislocated speckles are directly recorded as images on the specklegram, whereas the speckle dislocations in Fig. 2 are induced outside the test section by means of the defocusing of speckles formed outside the ground glass. In principle therefore the configuration presented in Fig. 3 can be free from an image blur since the specklegram dislocations can be recorded without defocusing the test section image. However, there will be no visible image of the test section in the recording plane, and the general optical alignment is more difficult. The field of depth of the camera must be shallow; otherwise the image can again be blurred owing to a vignetting bias of the test section image.

Another thing to note is that the speckle dislocation 0 increases with both the schlieren head magnification m and the camera magnification m' for the present system. For the case where a ground glass is placed after the test section (Fig. 2) the speckle dislocation increases with m' but decreases with m. Once the optical alignment is completed, the present configuration has a potential advantage over the previous configuration, at least in principle, in that the signal-to-noise ratio can be enhanced by simply increasing the camera magnification without the image blur.

Figure 4 schematically shows a refraction through a plane glass plate as an optical window attached to an experimental channel wall. The biasing ratio η can be defined as a fraction of the biased speckle dislocation because of the ray refractions through a glass plate of thickness t to the speckle dislocation that would result purely from the refractive-index field in the absence of the glass plate. Employing Snell's law[8] for refraction and assuming very small refraction angles, α and α', ,η can be

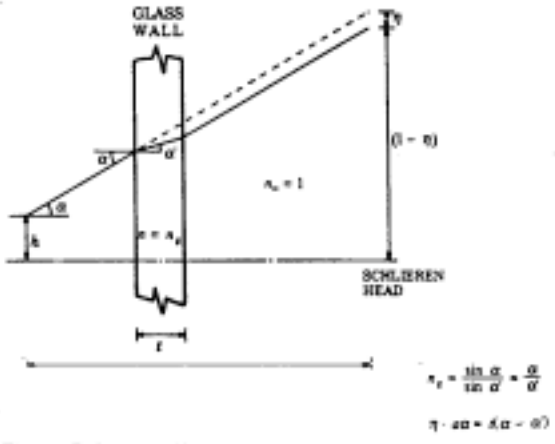

Fig. 4. Refraction of light rays through a glass plate of thickness t.

derived from the geometric consideration:

$$\eta = \frac{t}{a}\left(1 - \frac{1}{n_G}\right) \tag{6}$$

where t denotes the glass plate thickness and n_G represents the index of refraction of the glass. The biased speckle dislocation recorded on the actual specklegram will be equal to , $\eta \times \Delta$ for both cases presented in Figs. 2 and 3. To minimize the bias ratio η, the object distance a must be maximized. Since maximizing a for a given f reduces the magnification m, large values of a enhance the speckle dislocation amount for the system in Fig. 2 but reduce it for the system in Fig. 3. For most applications the biasing caused by the glass wall is negligibly small compared with the image biasing caused by the defocusing. For the optical configuration employed in the previous study,[4] for example, η, has been calculated to be 2.92 x 10^{-4} (a = 570 cm, t = 0.5 cm, and n_G = *1*.5), which is smaller than the image blur ratio from the defocusing ε by over an order of magnitude.

References

1. U. Wernekinck, and W. Merzkirch, "Measurement of natural convection by speckle photography," in *Proceedings of Heat Transfer 1986*, C. L. Tien, V. P. Carey, and J. K. Ferrel, eds. (Hemisphere, *Washington, D*.C., 1986), pp. 531-535.
2. W. Merzkirch, "Speckle photography," in *Handbook of Flow Visualization*, W. J Yang, ed. (Hemisphere, New York, 1989), Chap. 11.
3. D. Kastell, K. D. Kihm, and L. S. Fletcher, "Study of thermal boundary layers occurring around the leading edge of a vertical isothermal wall using speckle photography," Exp. Fluid (to be published).
4. K. D. Kihm, J. H. Kim, and L. S. Fletcher, "Effects of partial openings on natural convection heat transfer in triangular enclosures," in *Proceedings of the ASME Winter Annual Meeting* (American Society of Mechanical *Engineering, New* York, 1991), Heat Transfer Division. Vol. 177, pp. 51-57.
5. Y. Song, "Application of laser speckle photography in study of convective heat transfer," Ph.D. dissertation (Department of Engineering Mechanics, Tsinghua University, Beijing, China, 1988).
6. W. Merzkirch, *Flow Visualization* (Academic, New York, 1987), pp. 118-122.
7. R. J. Goldstein, "Optical technique for temperature measurement," in *Measurements in Heat Transfer*, E. R. G. Eckert and R. J. Goldstein, eds. (McGraw-Hill, New York, 1976), pp. 241-244.
8. E. Hecht, *Optics* (Addison-Wesley, Reading, Mass., 1987), p. 84.